

Hydrogen Peroxide-Responsive Nanoparticle Reduces Myocardial Ischemia/Reperfusion Injury

Soochan Bae, PhD; Minhyung Park, BA; Changsun Kang, BA; Serkan Dilmen, MD; Tae Hi Kang, PharmD; Dong Goo Kang, MD; Qingen Ke, MD; Seung Uk Lee, MD; Dongwon Lee, PhD; Peter M. Kang, MD

Background—During myocardial ischemia/reperfusion (I/R), a large amount of reactive oxygen species (ROS) is produced. In particular, overproduction of hydrogen peroxide (H_2O_2) is considered to be a main cause of I/R-mediated tissue damage. We generated novel H_2O_2 -responsive antioxidant polymer nanoparticles (PVAX and HPOX) that are able to target the site of ROS overproduction and attenuate the oxidative stress-associated diseases. In this study, nanoparticles were examined for their therapeutic effect on myocardial I/R injury.

Methods and Results—The therapeutic effect of nanoparticles during cardiac I/R was evaluated in mice. A single dose of PVAX (3 mg/kg) showed a significant improvement in both cardiac output and fraction shortening compared with poly(lactic-co-glycolic acid) (PLGA) particle, a non- H_2O_2 -activatable nanoparticle. PVAX also significantly reduced the myocardial infarction/area compared with PLGA (48.7 ± 4.2 vs 14.5 ± 2.1). In addition, PVAX effectively reduced caspase-3 activation and TUNEL-positive cells compared with PLGA. Furthermore, PVAX significantly decreased TNF- α and MCP-1 mRNA levels. To explore the antioxidant effect of PVAX by scavenging ROS, dihydroethidium staining was used as an indicator of ROS generation. PVAX effectively suppressed the generation of ROS caused by I/R, whereas a number of dihydroethidium-positive cells were observed in a group with PLGA I/R. In addition, PVAX significantly reduced the level of NADPH oxidase (NOX) 2 and 4 expression, which favors the reduction in ROS generation after I/R.

Conclusions—Taken together, these results suggest that H_2O_2 -responsive antioxidant PVAX has tremendous potential as a therapeutic agent for myocardial I/R injury. (*J Am Heart Assoc.* 2016;5:e003697 doi: 10.1161/JAHA.116.003697)

Key Words: antioxidant • inflammation • ischemia reperfusion injury • nanotechnology

Reactive oxygen species (ROS), such as superoxide anion, hydrogen peroxide (H_2O_2), and hydroxyl radical, are chemically reactive compounds that oxidize proteins, nucleic acids, and lipids.¹ ROS are derived from molecular oxygen and formed as a natural by-product of aerobic metabolism. Under normal circumstances, ROS are important secondary

messengers involved in multiple cellular signaling. The levels of ROS are controlled by antioxidants, which keep them in the picomolar range.² However, accumulation of ROS over extended periods of time causes oxidative stress, which triggers cell death and irreversible tissue damage. Many diseases are associated with ROS-mediated oxidative stress, including cancer, neurodegenerative diseases, and I/R injury. In particular, ROS overproduction is one of the central pathological mechanisms in cardiac I/R injury.³ It is well accepted that a large amount of ROS is generated immediately after reperfusion and may elicit cell death, such as apoptosis.^{4,5}

Among various ROS, superoxide anion and H_2O_2 are particularly important in cardiomyocytes. Superoxide anion is short-lived and is rapidly reduced to H_2O_2 spontaneously or by superoxide dismutase. In contrast, H_2O_2 has a longer biological life span and is easily diffusible within and between cells.⁶ A massive accumulation of H_2O_2 is known to be the critical pathogenic mechanism of I/R-induced tissue damage by releasing proinflammatory cytokines and triggering apoptosis.⁷ In this context, targeting the site of H_2O_2 overproduction and rapid reduction of excessive ROS are promising strategies to alleviate myocardial I/R injury.^{4,8} Numerous

From the Cardiovascular Institute, Beth Israel Deaconess Medical Center, Boston, MA (S.B., M.P., C.K., S.D., T.H.K., D.G.K., Q.K., P.M.K.); Harvard Medical School, Boston, MA (S.B., M.P., C.K., S.D., T.H.K., D.G.K., Q.K., P.M.K.); Department of BIN Fusion Technology, Chonbuk National University, Jeonju, South Korea (M.P., C.K., D.L., P.M.K.); Department of Cardiology, Gwangju Christian Hospital, Gwangju, South Korea (D.G.K., S.U.L.).

Correspondence to: Peter M. Kang, MD, Cardiovascular Institute, Beth Israel Deaconess Medical Center, 3 Blackfan Circle, CLS 910, Boston, MA 02215. E-mail: pkang@bidmc.harvard.edu and Dongwon Lee, PhD, Department of BIN Convergence, Chonbuk National University, Dukjin, Jeonju 561-756, South Korea. E-mail: dlee@jbnu.ac.kr

Received April 7, 2016; accepted September 28, 2016.

© 2016 The Authors. Published on behalf of the American Heart Association, Inc., by Wiley Blackwell. This is an open access article under the terms of the Creative Commons Attribution-NonCommercial License, which permits use, distribution and reproduction in any medium, provided the original work is properly cited and is not used for commercial purposes.

antioxidants have been explored as therapeutic agents for I/R injuries.⁸ Various formulations of nanoparticles have also been developed as drug carriers that could release the drug payloads in spatial and temporal-specific manners to enhance their therapeutic efficacy.^{9,10}

Recently, we have developed H₂O₂-responsive antioxidant copolyoxalates containing hydroxybenzyl alcohol (HBA) (HPOX) and vanillyl alcohol (VA) (PVAX) that could serve as therapeutic agents for ROS-associated diseases.^{11,12} PVAX or HPOX was synthesized using naturally occurring compounds with intrinsic antioxidant and anti-inflammatory activities, VA and HBA, respectively. These polymers were chemically engineered to possess H₂O₂-responsive peroxalate ester linkages and therapeutic agents in their backbone. These antioxidant polymeric prodrug nanoparticles have a mean diameter of ~400 nm. They could be rapidly activated by H₂O₂ at the site of ROS generation. They prevent the I/R-induced injuries by exerting antioxidant, anti-inflammatory, and antiapoptotic effects.^{11,12} Their therapeutic effects were explained by the synergistic effects of H₂O₂-scavenging peroxalate ester bonds with antioxidant and anti-inflammatory effects of therapeutic agents (VA or HBA).^{11,12} However, direct comparison between HPOX and PVAX has not been made, and their potential as therapeutic agents for myocardial I/R injury has not been evaluated. The objective of the present work is to evaluate the potential of antioxidant copolyoxalates as therapeutic agents for myocardial I/R injury. We first used a mouse model of hind limb I/R to directly compare their therapeutic effects on I/R injury. The direct comparison studies revealed that PVAX has superior therapeutic and protective effects against I/R compared to HPOX. We then utilized a mouse cardiac I/R injury model to determine the potential of PVAX as a therapeutic agent.

Methods

Synthesis of PVAX and HPOX

PVAX was synthesized using 1,4-cyclohexanedimethanol (21.96 mmol), 4-vanillyl alcohol (VA, 5.49 mmol), and oxalyl chloride (27.45 mmol). HPOX was synthesized using 1,4-cyclohexanedimethanol (21.96 mmol), and 4-hydroxybenzyl alcohol (HBA, 5.49 mmol), and oxalyl chloride (27.45 mmol) in dry dichloromethane.

Preparation and Administration of PVAX and HPOX Nanoparticles

HPOX or PVAX nanoparticles were generated using an emulsion/solvent evaporation method as previously reported.^{11,12} In brief, HPOX or PVAX dissolved in DCM was added to 5 mL of 10% (w/v) polyvinyl alcohol (PVA) solution. The mixtures were

sonicated and then homogenized to form fine oil/water emulsions. The emulsion was transferred to a 20-mL PVA (1% w/v) solution and homogenized for another 1 minute. The remaining solvent was removed using a rotary evaporator. The particles were then centrifuged and washed with deionized water 3 times to remove the residual PVA. The suspension was then frozen in liquid nitrogen and lyophilized to produce free-flowing particles. One milligram of HPOX or PVAX was dissolved in 1 mL of phosphate-buffered saline (PBS). PVAX or HPOX was administered into the gastrocnemius muscles in hind limb I/R injury model. PVAX was administered intraperitoneally in the cardiac I/R injury model.

Sensitivity of PVAX and HPOX to H₂O₂

For the evaluation of H₂O₂ scavenging ability, 1 mg of PVAX or HPOX nanoparticles was added in 1 mL of 10 μmol/L H₂O₂ solution. One minute after the addition, the concentration of H₂O₂ solution was determined using the Amplex Red assay kit (Invitrogen, Carlsbad, CA). For the H₂O₂ sensitivity assay, rubrene-loaded PVAX or HPOX nanoparticles were prepared as previously reported.^{11,12} The chemiluminescent nanoparticles were added in H₂O₂ solutions with various concentrations. The chemiluminescent intensity was measured using a luminometer (Femtomaster FB12, Zylux Corp, Huntsville, AL).

Flow Cytometry

RAW264.7 cells were cultured for 24 hours in a 24-well culture plate prior to the experiments. Cells were treated with 100 μg of PVAX or HPOX nanoparticles for 6 hours, and then intracellular ROS generation was induced by treatment with 1 μg of phorbol-12-myristate-13-acetate (PMA). For the detection of ROS, the cell suspensions were transferred to a 5-mL culture tube and stained with 5 μmol/L dichlorofluorescein diacetate (DCFH-DA), followed by gentle mixing. Apoptotic cell death was induced by the addition of 300 μmol/L of H₂O₂. For the analysis of apoptosis, the cell suspensions were treated with Annexin V-FITC. The stained cells were analyzed by flow cytometry (FACS Calibur, Becton Dickinson, San Jose, CA). A total of 1.0 × 10⁴ events were counted for each sample.

Animal Surgeries

Animal surgeries were performed in 12- to 13-week-old male C57/B mice (Charles River Laboratory, Wilmington, MA). For hind limb I/R surgery, a femoral artery was identified and tied around a specialized 30G catheter with a 7-0 silk suture after mice were anesthetized with inhalant isoflurane (2%). Full anesthesia was verified with toe pinching. The animal

remained under anesthesia for a specified duration of ischemia. Reperfusion was achieved by cutting the suture and reestablishing arterial blood flow. Sham-operated mice underwent the same procedure without the femoral artery occlusion/reperfusion. For cardiac I/R surgery, mice were anaesthetized, intubated, and placed on a rodent ventilator (model 687, Harvard Respirator). After thoracotomy, the left anterior descending artery (LAD) artery was identified and ligated with a 7-0 silk suture tied around a specialized 30G catheter. The animal remained under anesthesia and ventilation for 45 minutes of ischemia. Reperfusion was achieved by cutting the suture and reestablishing arterial perfusion. Sham-operated mice underwent the same procedure without LAD occlusion and reperfusion. Mice were sacrificed by heart extraction after anesthetizing with inhalant isoflurane (2%). Animal experiments performed conform to the NIH guidelines (*Guide for the Care and Use of Laboratory Animals*) on the protection of animals used for scientific purposes. All experimental procedures were approved by the Institutional Animal Care and Use Committee of Beth Israel Deaconess Medical Center.

Cardiac Functional Analysis

Cardiac function was measured in mice using the left ventricle (LV) pressure-volume loop and echocardiography 2 weeks after I/R surgery or sham control. After 2% isoflurane inhalant anesthesia, the pressure-volume parameters were measured using a 1.4Fr microtip pressure-volume catheter (ScisenseInc, Ontario, Canada). The catheter was first inserted into the right common carotid artery and then gently advanced into the LV to obtain LV hemodynamic parameters. Data were recorded using a Powerlab system (ADInstruments, Colorado Springs, CO). Beat-by-beat pressure-volume parameters including heart rate (HR), stroke volume (SV), stroke work (SW), and cardiac output (CO) were measured and analyzed using CardioSoft Pro software (CardioSoft, Houston, TX). Transthoracic echocardiography was performed using a Vevo2100 echocardiogram (VisualSonics, Toronto, Canada) with a MS400 (18–38 MHz) transducer at baseline and 2 weeks after I/R. Two-dimensional guided M-mode images were recorded.

Infarct Size Determination

Infarct size was measured 24 hours after I/R surgery as described previously.¹³ After thoracotomy, the LAD was religated, and 50 μ L green fluorescent FluoSpheres (Molecular Probe, Carlsbad, CA) was injected into the LV of the heart to delineate the area at risk (FluoSpheres-negative area). The heart was then excised, fixed, and sectioned into 1-mm perpendicular sections. Sections were stained with 2,3,5-

triphenyltetrazolium chloride (TTC) (Sigma Chemical, St. Louis, MO) solution to determine the infarcted myocardium (TTC-negative area). The infarction area (IA) and the area at risk (AAR) were determined for each slice using a computer planimetry and NIH Image software.

Reverse Transcriptase-Polymerase Chain Reaction Analysis for mRNA Expression

Heart tissues were collected for molecular analysis after I/R. Reverse transcriptase-polymerase chain reaction (RT-PCR) was performed as described previously.^{11,12} The mRNA expression levels were analyzed by RT-PCR using specific primers. Ribosomal 18S primers acted as internal controls, and all RT-PCR signals were normalized to the 18S signal of the corresponding RT product to eliminate the measurement error from uneven sample loading and to provide a semi-quantitative measure of the relative changes in gene expression. The PCR primers used in this study are listed below: sense TNF- α , 5-CCTCAG CCTCTTCTCCTTCT-3; antisense TNF- α , 5-GGTGTGGGTGAGGAGCA-3; sense MCP-1, 5-CCC CACTCACCTGCTGCTACT-3; antisense MCP-1, 5-GCATCAGAGTCCGAGTCACA -3; sense 18S, 5-GTTATGGTTCCTTTGT CGCTCGCTC-3, anti-sense 18S, 5-TCGGCCCCGAGGTTATCTAGAGTCAC-3.

Caspase-3 and PARP Activity Assay

The activity of caspase-3 was determined with a colorimetric assay kit (R&D Systems, Minneapolis, MN) as described previously.^{11,12} Briefly, protein samples were added to the substrates of Acetyl-Asp-Glu-Val-Asp-p-nitroanilide. The enzyme-catalyzed release of p-nitroanilide was measured at 405 nm. For PARP activity assay, activity was measured at 450 nm for incorporation of biotinylated poly(ADP-ribose) onto histone-coated proteins in a plate using a colorimetric assay kit (R&D Systems, Minneapolis, MN) as described previously.¹¹

Terminal Deoxynucleotidyl Transferase dUTP Nick End Labeling Staining and Dihydroethidium Staining

Terminal deoxynucleotidyl transferase dUTP nick-end labeling (TUNEL) staining was performed using an in situ cell death detection kit, fluorescein (Roche Applied Science, Indianapolis, IN) as described previously.^{11,12} To distinguish cardiomyocyte from noncardiomyocyte nuclei, we used triple staining for nuclei (4',6-diamidino-2-phenylindole [DAPI] staining), apoptotic nuclei (TUNEL staining), and cardiomyocytes (α -actinin staining) and analyzed the stained sections using confocal microscopy. For dihydroethidium (DHE)

staining, tissue sections were incubated with 5 $\mu\text{mol/L}$ of DHE (Sigma-Aldrich, St. Louis, MO) at 37°C for 30 minutes in a humidified chamber protected from light, and then DAPI was applied. Images were acquired by confocal fluorescent microscope.

Western Immunoblot

NADPH oxidase 2 (NOX2) and NOX4 proteins were probed with an anti-NOX2 and anti-NOX4 rabbit monoclonal antibody (Abcam, Cambridge, MA). Glyceraldehyde 3-phosphate dehydrogenase (GAPDH) was used as an internal control for loading. Resulting bands were quantified as optical density (OD) \times band area by ImageJ analysis system and recorded as arbitrary units.

Primary Adult Rat Ventricular Cardiomyocyte Culture

The primary culture of adult rat ventricular cardiomyocytes (ARVC) was prepared from the hearts of female rats as described previously.¹⁴ Rat hearts were extracted after anesthesia with inhalant isoflurane (2%). For cell viability, a 3-(4,5-dimethylthiazil-2yl)-2,5-diphenyltetrazolium bromide (MTT) assay was performed according to the manufacturer's instructions (Sigma, St. Louis, MO), and as previously reported.¹⁴ Briefly, cells were treated with MTT for 3 hours. Formed formazan crystals were dissolved with dimethyl sulfoxide while plates were agitated on a shaker for 30 minutes in the dark. Absorbance was measured at 570 nm with a reference wavelength at 690 nm.

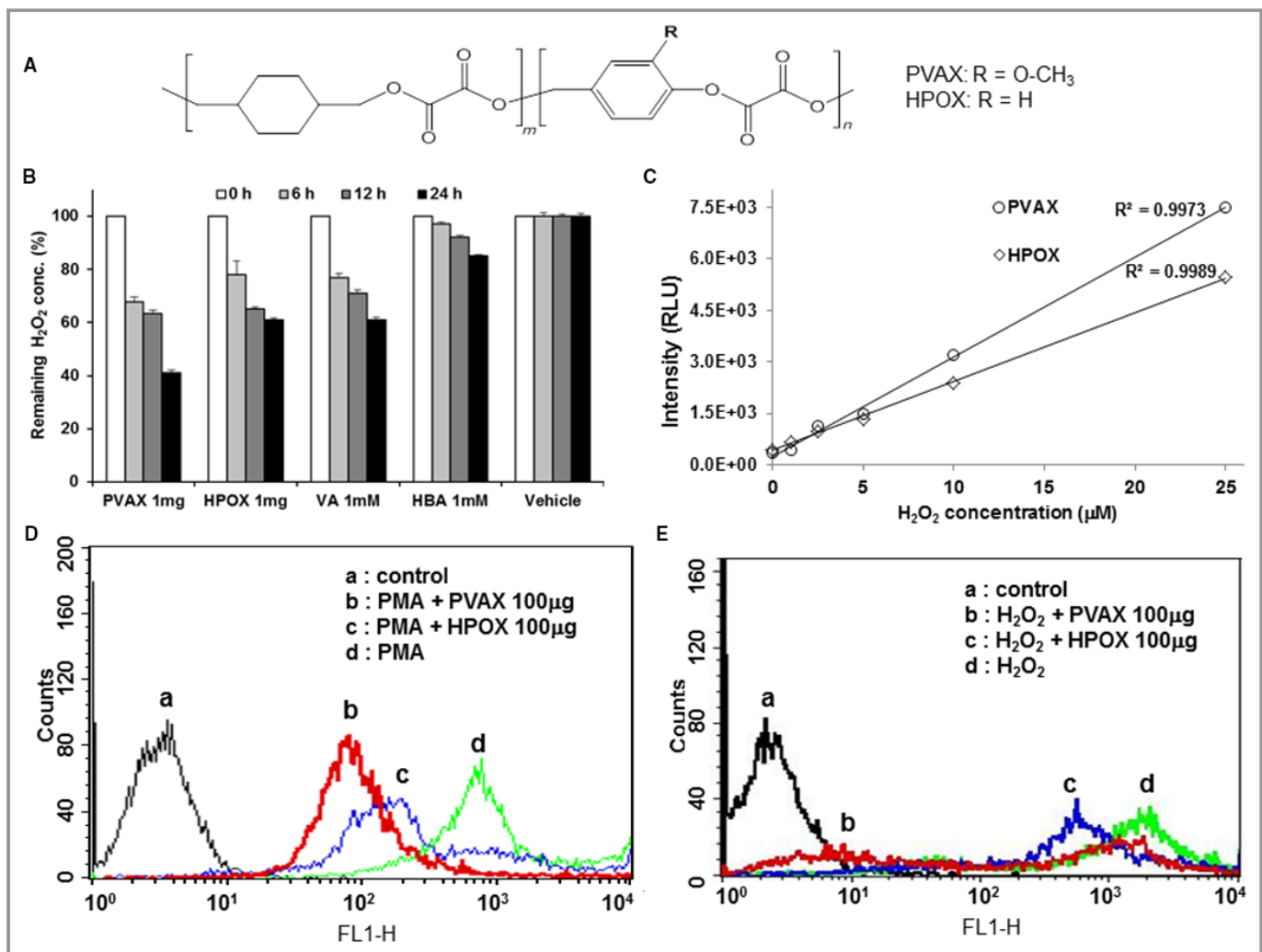


Figure 1. Chemical and biological properties of PVAX and HPOX nanoparticles. A, Chemical structure of antioxidant copolyoxalates, PVAX and HPOX. B, Scavenging of H₂O₂ by PVAX and HPOX nanoparticles. C, Sensitivity of PVAX and HPOX nanoparticles to H₂O₂ based on peroxalate chemiluminescence. D, Inhibitory effects of PVAX and HPOX nanoparticles on ROS generation in PMA-stimulated cells. E, Inhibitory effects of PVAX and HPOX nanoparticles on H₂O₂-induced apoptotic cell death. PMA indicates phorbol-12-myristate-13-acetate; ROS, reactive oxygen species.

Statistical Analyses

Data were expressed as means±SEM. For continuous data following a normal distribution, differences between two groups were analyzed by an unpaired 2-tailed Student *t* test. Differences among more than 2 groups were analyzed by 1-way ANOVA with Bonferroni post hoc test. For data not following a normal distribution, differences between 2 groups were analyzed by Mann-Whitney test, and multiple groups by Kruskal-Wallis test. R² values provide linear relationship between 2 groups. All the statistics were calculated using GraphPad Prism 5.0 (San Diego, CA). Probability (*P*) values of <.05 were considered significant.

Results

H₂O₂-Responsiveness of PVAX and HPOX

PVAX and HPOX were synthesized as H₂O₂-responsive antioxidant polymeric prodrugs of VA and HBA, respectively (Figure 1A). Both polymers had average molecular weights of ~15 000 Da and formed nanoparticles with mean diameters of ~400 nm with smooth surfaces.^{11,12} Although there was no change in H₂O₂ concentration at each time

point in the vehicle control, both PVAX and HPOX nanoparticles (1 mg/mL) significantly eliminated H₂O₂ in a time-dependent manner (Figure 1B). However, PVAX nanoparticles showed a stronger H₂O₂-scavenging ability than HPOX nanoparticles. The stronger H₂O₂-scavenging ability of PVAX nanoparticles over HPOX nanoparticles can be explained by the superior H₂O₂-scavenging ability of VA, which may be due to the presence of a methoxy group.¹⁵ Their sensitivity to H₂O₂ was also evaluated based on peroxalate chemiluminescence. Rubrene as a fluorophore was encapsulated in the PVAX and HPOX nanoparticles, and the chemiluminescent nanoparticles were added into H₂O₂ solutions of various concentrations. Both chemiluminescent nanoparticles showed a linear correlation between chemiluminescence intensity and H₂O₂ concentration (Figure 1C). However, PVAX nanoparticles showed higher emission intensity than HPOX nanoparticles.

In addition, we compared the antioxidant and antiapoptotic activities of PVAX and HPOX nanoparticles in vitro. RAW264.7 cells were stimulated with PMA to induce ROS generation (Figure 1D). The generation of ROS in PMA-stimulated cells was investigated using a ROS probe, DCFH-DA, which becomes fluorescent on activation by ROS such as

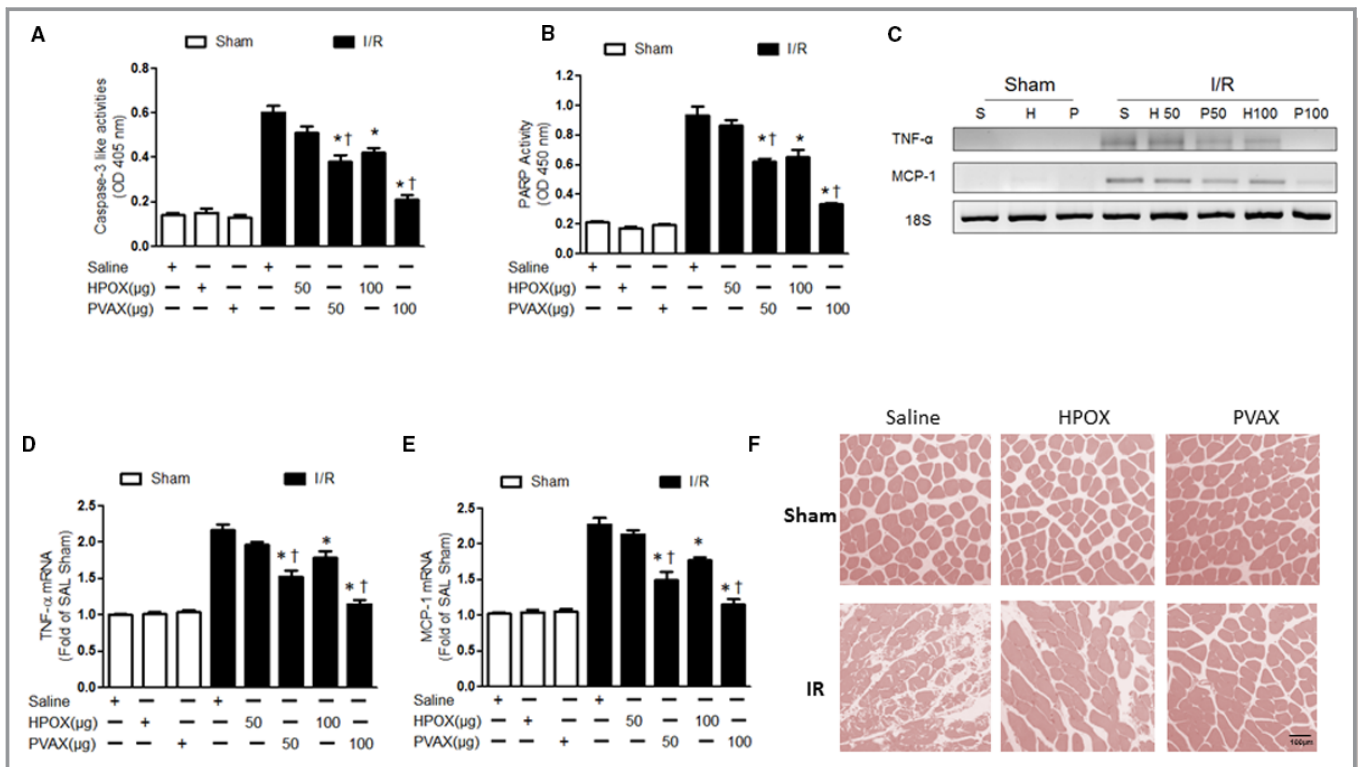


Figure 2. The therapeutic effects of PVAX and HPOX nanoparticles on hind limb I/R injury. A and B, Quantification of caspase-3 (A) and PARP activity (B) **P*<0.05 vs sham of each group; †*P*<0.05 vs HPOX I/R. (n=4/group). Mann-Whitney test was used. C, Expression of inflammatory markers TNF-α and MCP-1 in hind limb I/R injury. D and E, Quantification of TNF-α (D) and MCP-1 (E) mRNA level, **P*<0.05 vs sham of each group; †*P*<0.05 vs HPOX I/R. (n=4/sham group, n=6/I/Rgroup). ANOVA and Bonferroni test were used. F, Representative images of gastrocnemius muscle tissues stained by hematoxylin and eosin (×200). I/R indicates ischemia/reperfusion; MCP-1, monocyte chemoattractant protein-1; TNF-α, tumor necrosis factor-α.

H₂O₂ and hydroxyl radical. Both HPOX and PVAX showed decreases in their fluorescent intensity compared to the PMA alone, but PVAX induced a greater reduction in the fluorescence intensity than HPOX, indicating that PVAX have more inhibitory effects on PMA-induced ROS generation. Antiapoptotic effects of both nanoparticles on H₂O₂-stimulated cells were evaluated by staining with annexin V-FITC as a marker of apoptosis (Figure 1E). PVAX again exerted stronger antiapoptotic activity in H₂O₂-stimulated cells than HPOX.

Comparison of PVAX and HPOX Using a Mouse Model of Hind Limb I/R Injury

To compare antiapoptotic and anti-inflammatory activities of HPOX and PVAX nanoparticles, a mouse model of hind limb I/R injury was used. I/R injury was induced by tying the femoral artery with a suture for 1 hour, followed by reperfusion. PVAX and HPOX (50 and 100 μg) were directly injected just distal to the ligation site, and their therapeutic effects were compared by measuring the level of anti-inflammatory and antiapoptotic activities. The activities of caspase-3 and polyADP ribose polymerase (PARP) were analyzed to measure the level of apoptosis. I/R injury caused significant elevation of caspase-3 and PARP activities (Figure 2A and 2B). Both PVAX and HPOX

nanoparticles significantly decreased the activities of caspase-3 and PARP in a dose-dependent manner. However, PVAX showed significantly greater antiapoptotic activity than HPOX. The levels of tumor necrosis factor-α (TNF-α) and monocyte chemotactic protein-1 (MCP-1) were evaluated as markers of inflammation. Both nanoparticles significantly suppressed I/R-induced expression of mRNA of TNF-α and MCP-1 (Figure 2C through 2E). In particular, 100 μg of PVAX almost completely suppressed the expression of mRNA of TNF-α and MCP-1. In addition, H&E staining demonstrated that muscle damage caused by I/R injury was significantly inhibited by PVAX (Figure 2F). Based on these findings, we conclude that PVAX has superior anti-inflammatory and antiapoptotic activities against ROS-associated diseases than HPOX. Thus, PVAX was selected as a therapeutic agent for subsequent cardiac I/R injury experiments.

Therapeutic Effects of PVAX Nanoparticles on H₂O₂-Stimulated Adult Rat Cardiomyocytes

First, antioxidant and anti-inflammatory activities of PVAX nanoparticles were studied using the primary culture of adult rat cardiomyocytes (ARVC). To test protective effect of PVAX against oxidative stress in vitro, we examined H₂O₂-induced

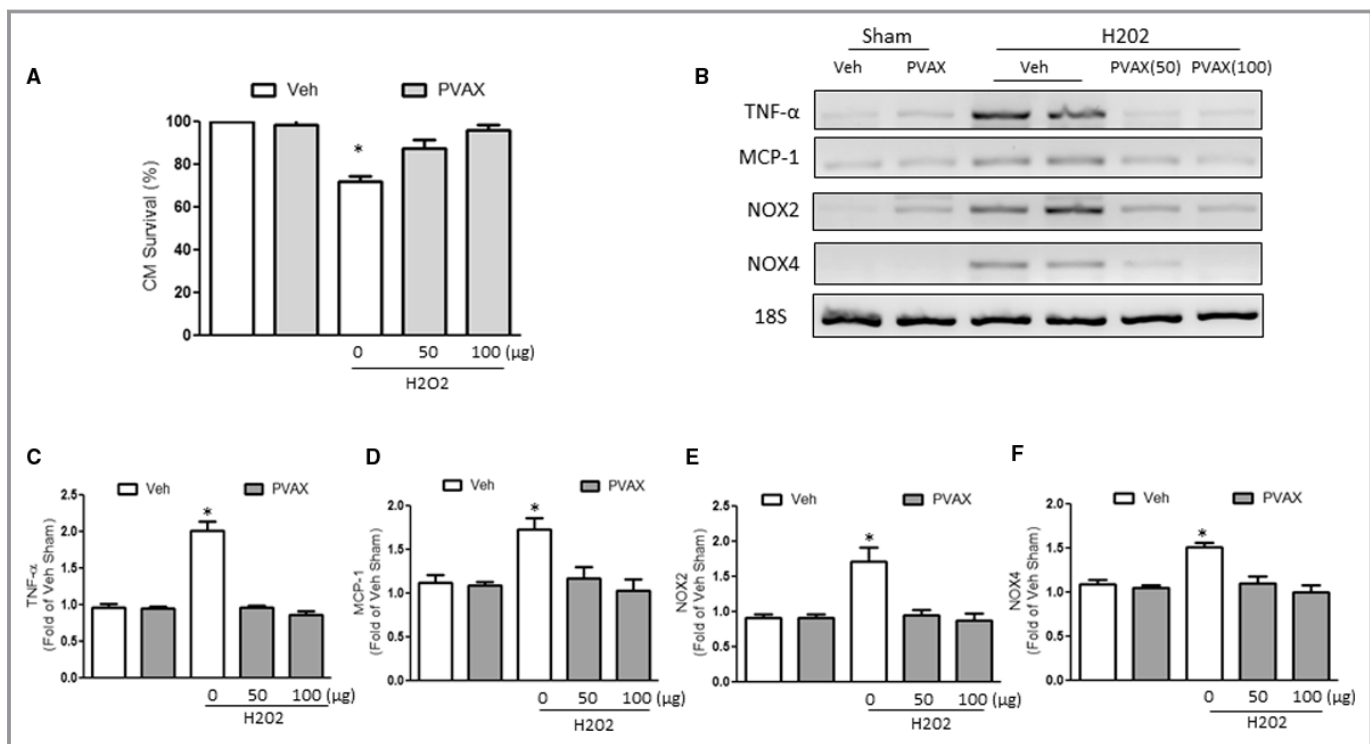


Figure 3. The therapeutic effect of PVAX on H₂O₂-stimulated adult rat cardiomyocytes in vitro. A, Protective effects of PVAX nanoparticles on H₂O₂-stimulated cardiomyocytes. (n=3/group). Mann-Whitney test was used. B, Expression of TNF-α and MCP-1. The images are representatives of 4 experiments. C through F, Quantification of TNF-α (C), MCP-1 (D), NOX2 (E), and NOX4 (F). **P*<0.05 vs sham of each group. (n=4/group). The Mann-Whitney test was used. MCP-1 indicates monocyte chemotactic protein-1; NOX2, NADPH oxidase 2; NOX4, NADPH oxidase 4; TNF-α, tumor necrosis factor-α.

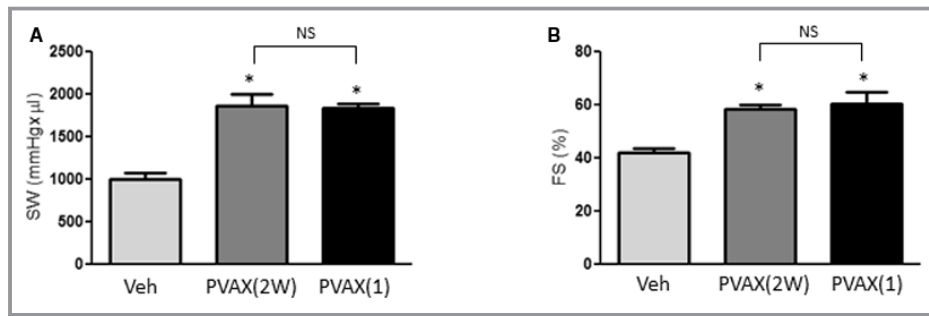


Figure 4. Effect of different PVAX nanoparticle administration methods on I/R-induced cardiac dysfunction. A and B, Cardiac functions after I/R were evaluated after vehicle (Veh), daily injection of PVAX (3 mg/kg per day for 2 weeks) (2W), or single injection of PVAX (3 mg/kg) (1). Stroke work (SW) (A) was determined using PV loop analysis. Fractional shortening (FS) (B) was measured using echocardiography. **P*<0.05 vs Veh. NS=not significant (n=6/veh, n=4/PVAX 2W and 1 group). The Kruskal-Wallis and Dunn tests were used. I/R indicates ischemia/reperfusion.

cell death in ARVC. Compared to the vehicle control, PVAX showed significant protection from H₂O₂-induced cell death in a concentration dependent manner (Figure 3A). Treatment

with H₂O₂ (250 μmol/L) significantly increased expression of inflammatory markers, such as TNF-α, MCP-1, NOX2, and NOX4 (Figure 3B through 3F). PVAX treatment effectively

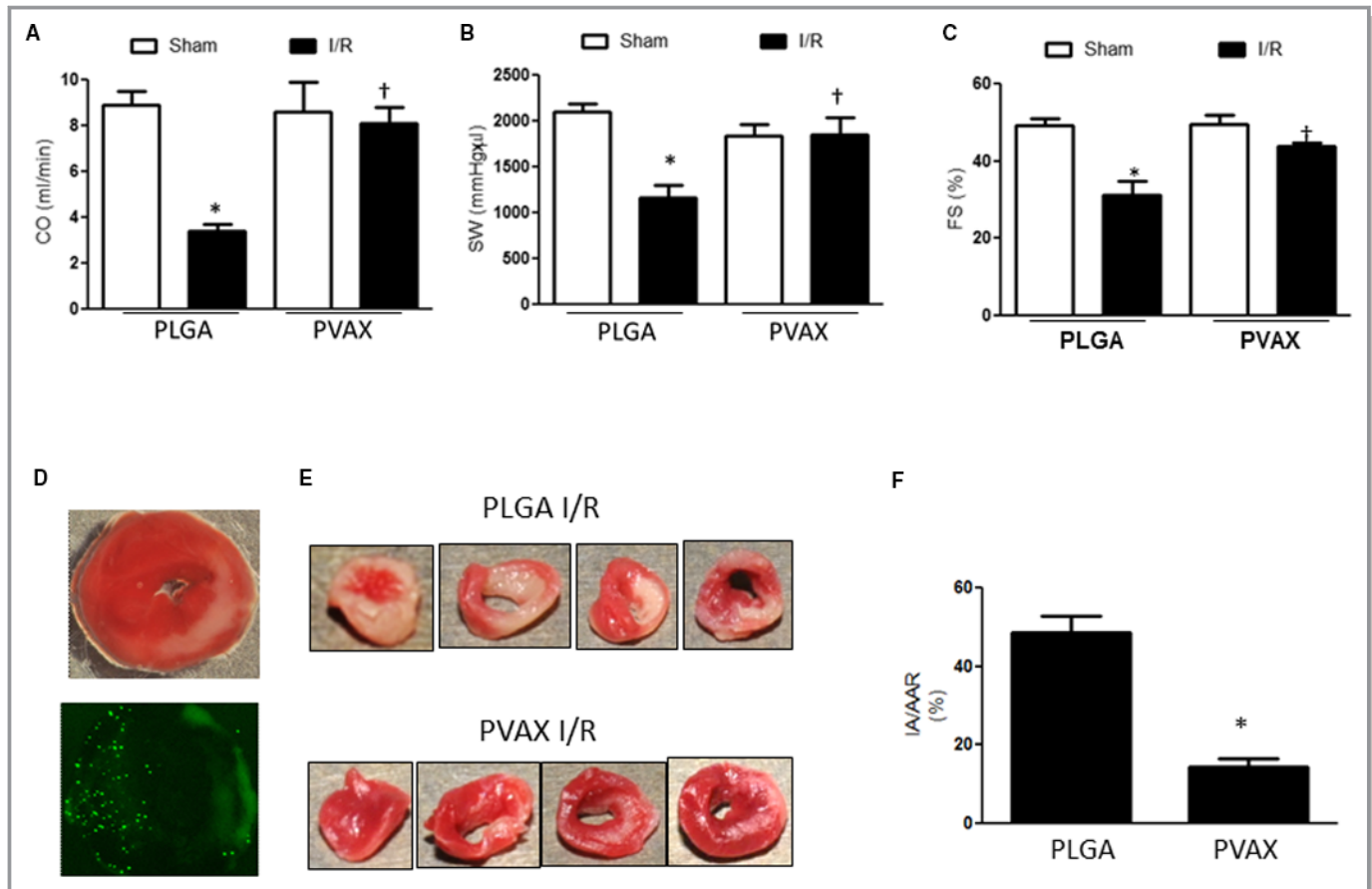


Figure 5. Effect of PVAX and PLGA nanoparticles on I/R-induced cardiac dysfunction. A, Cardiac output (CO), (B) stroke work (SW), and (C) fractional shortening (FS) 2 weeks after I/R in mice after PLGA or PVAX (3 mg/kg, single injection). **P*<0.05 vs sham of each group; †*P*<0.05 vs PLGA I/R. (n=5/sham group, n=6/I/R group). ANOVA and a Bonferroni test were used. D, Representative images of heart tissues after I/R injury after TTC staining (top) or fluorescent microspheres administration (bottom). E, Representative heart tissue sections stained with TTC solution. Red-colored regions in the TTC-stained sections indicate nonischemic areas; pale-colored regions indicate ischemic portions of the heart. F, Quantification of infarction area (IA)/area at risk (AAR) **P*<0.05 (n=4/PLGA, n=5/PVAX). Student t test was used. I/R indicates ischemia/reperfusion; TTC, triphenyltetrazolium chloride.

blocked the H₂O₂-induced TNF- α , MCP-1, NOX2, and NOX4 activation.

Therapeutic Effects of PVAX Nanoparticles on Cardiac Functions After I/R Injury

Because reperfusion of the ischemic myocardium triggers further production of ROS causing myocardial dysfunction, we evaluated the beneficial effects of H₂O₂-responsive PVAX nanoparticles using a mouse model of cardiac I/R injury. Previous studies have demonstrated that cardiac function is decreased 2 weeks after I/R injury.^{16–18} Thus, the cardiac functions were evaluated 2 weeks after cardiac I/R injury using PV loop analysis and echocardiogram. The overproduction of ROS at the time of reperfusion is the critical time when the tissue injuries likely occur, so we initially compared single administration of PVAX (3 mg/kg) 10 minutes before reperfusion with daily injection of PVAX (3 mg/kg per day). Interestingly, single administration of PVAX (3 mg/kg) was comparable

to daily injection of PVAX in terms of attenuating cardiac dysfunction (Figure 4A and 4B). Therefore, we chose single-dose administration of PVAX for our further experiments.

Next, the beneficial effects of PVAX after cardiac I/R were compared with poly(lactic-co-glycolic acid) (PLGA) nanoparticles, which have no H₂O₂ responsiveness, as a vehicle comparison. Administration of PLGA nanoparticles before reperfusion did not improve I/R-induced cardiac dysfunction when evaluated with PV loop and echocardiography analyses (Figure 5A through 5C). There was no mortality after I/R surgery in both PLGA and PVAX I/R groups. However, significant differences of cardiac function parameters were observed between PVAX- and PLGA-treated animals after I/R. In addition, we evaluated infarct size 24 hours after I/R. Consistent with cardiac function evaluation, PVAX nanoparticles significantly reduced the infarct size compared with the PLGA group (48.7 ± 4.2 vs 14.5 ± 2.1 , $P < 0.05$) (Figure 5D through 5F).

Cell death and inflammation are important mechanisms involved in cardiac I/R injury. To determine whether the

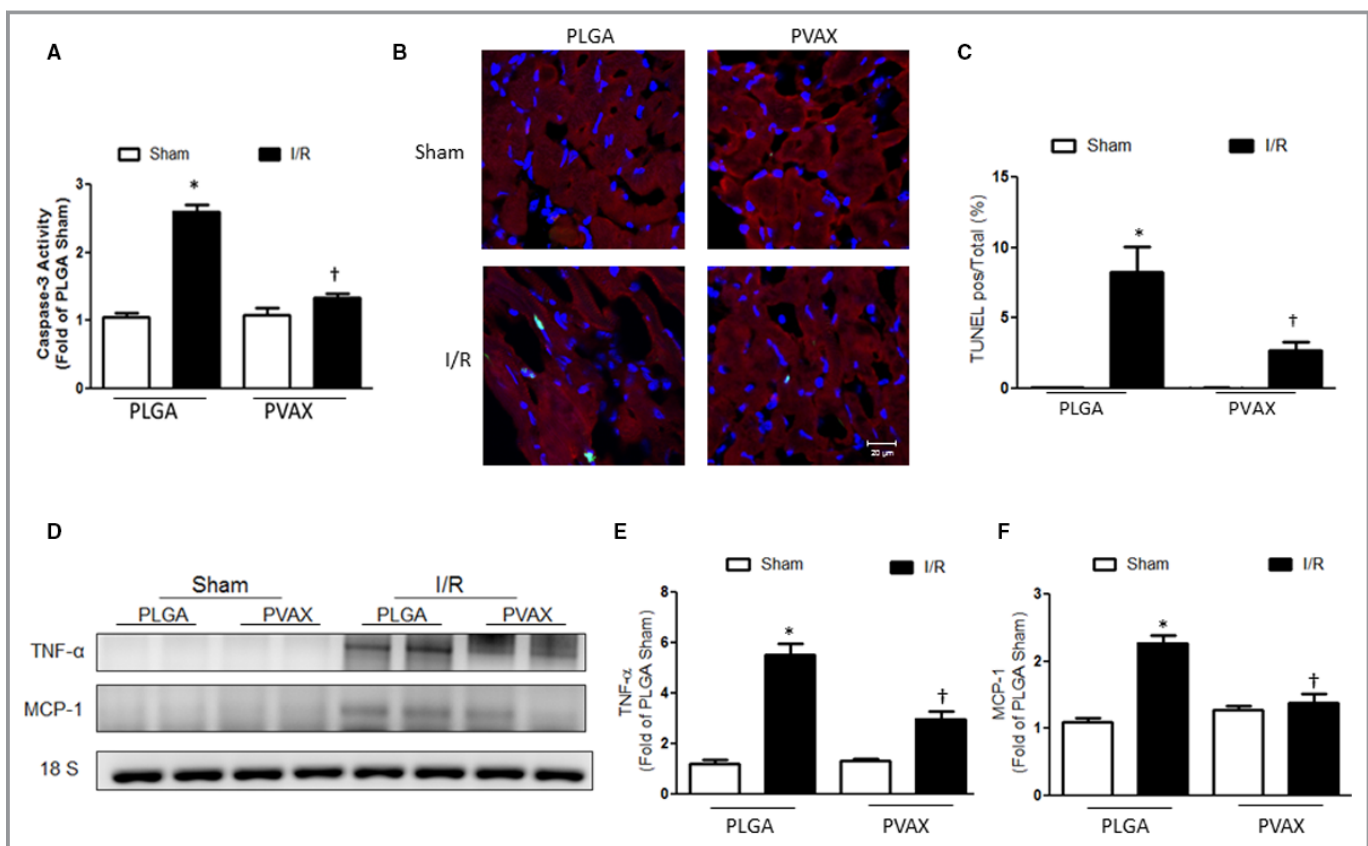


Figure 6. Anti-inflammatory and antiapoptotic activities of PVAX nanoparticles after cardiac I/R injury. A, Quantification of caspase-3 activity assay. * $P < 0.05$ vs sham of each group; † $P < 0.05$ vs PLGA I/R (n=4/sham group, n=5 per I/R group). ANOVA and a Bonferroni test were used. B, Representative images of TUNEL staining. TUNEL, green; nuclei, blue; α -actinin, red. C, Quantification of TUNEL-positive cells/total cells. * $P < 0.05$ vs sham of each group; † $P < 0.05$ vs PLGA I/R. (n=4/sham group, n=5 per I/R group). ANOVA and a Bonferroni test were used. D, Expression of inflammatory markers TNF- α and MCP-1. E and F, Quantification of TNF- α (E) and MCP-1 (F) mRNA level. * $P < 0.05$ vs sham of each group; † $P < 0.05$ vs PLGA I/R. (n=4/sham group, n=5 per I/R group). ANOVA and a Bonferroni test were used. I/R indicates ischemia/reperfusion; TUNEL, terminal deoxynucleotidyl transferase dUTP nick-end labeling; TNF- α , tumor necrosis factor- α .

beneficial effects of PVAX nanoparticles are associated with their antiapoptotic and anti-inflammatory activities, we examined the level of apoptosis and inflammation after I/R. PVAX significantly reduced caspase-3 activation and the TUNEL-positive cells after I/R compared to the PLGA-treated group (Figure 6A and 6B). In addition, PVAX significantly decreased TNF- α and MCP-1 mRNA expressions compared to I/R in PLGA mice (Figure 6C through 6E). These results indicate that PVAX effectively prevents I/R-induced damage by inhibiting inflammation and apoptosis.

Effects of PVAX on NOX-Induced ROS Generation After Cardiac I/R

Recent studies show that NOX-derived ROS plays a pivotal role in cardiac I/R. The increased level of NOX activity/expression and NOX-dependent ROS production influence several key components of cardiac remodeling, such as myocyte hypertrophy, contractile dysfunction, apoptosis, and fibrosis.¹⁹ To investigate antioxidant activities of PVAX, heart tissues were stained with DHE as a fluorescent marker of ROS. A number of DHE-positive cells were observed in a PLGA I/R group, indicating that I/R injury induced a large generation of ROS. PVAX nanoparticles effectively reduced the generation of ROS caused by I/R (Figure 7A). We also investigated the effects of PVAX nanoparticles on the

expression of NOX2 and NOX4 24 hours after reperfusion. The levels of NOX2 and NOX4 were elevated after I/R (Figure 7B through 7D). However, PVAX nanoparticles significantly reduced the levels of NOX2 and NOX4 compared to PLGA nanoparticles. These results suggest that the reduction of ROS production is attributed to the blockade of NOX2 and NOX4 expression.

Discussion

Although mechanisms of cardiac I/R injury are complex, ROS are major initiators of myocardial damage during I/R. With an elevated level of ROS, cells experience oxidative stress, which then could lead to irreversible damages due to proinflammatory cytokine release, apoptosis, and interstitial fibrosis. Among various ROS, H₂O₂ is the most abundant and critical for redox signaling because of its long half-life and diffusion distance (~1-1600 μ m).⁶ In particular, overproduction of H₂O₂ is an important pathogenic mechanism of I/R-induced tissue damage through an increase in proinflammatory cytokines such as TNF- α , through activation of p38 MAPK.²⁰ Excessive ROS after reperfusion also resulted in a marked increase in infarct size, and counteracting the ROS generation reduced the infarct size by up to 50%.⁶ Thus, great efforts have been made to develop therapeutic strategies to attenuate I/R injury by suppressing ROS generation and inflammation.^{13,21-23}

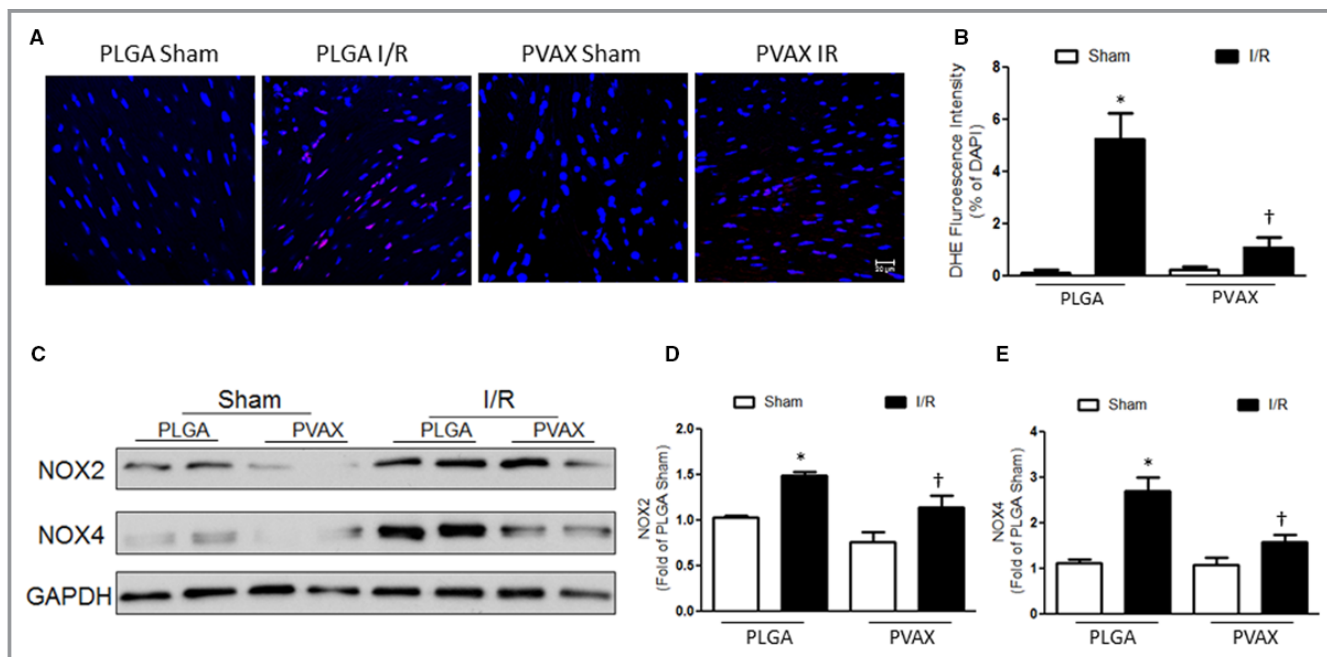


Figure 7. Antioxidant activities of PVAX nanoparticles after cardiac I/R injury. A, Representative image of DHE staining. DHE=red, nuclei=blue. B, Quantification of DHE-positive nuclei. * $P<0.05$ vs sham of each group; † $P<0.05$ vs PLGA I/R (n=4/sham group, n=5 per I/R group). ANOVA and a Bonferroni test were used. C, Representative images of mRNA expression of NOX2 and NOX4. D and E, Quantification of NOX2 (D) and NOX4 (E) expression. * $P<0.05$ vs sham of each group; † $P<0.05$ vs PLGA I/R (n=4/sham group, n=5 per I/R group). ANOVA and a Bonferroni test were used. DHE indicates dihydroethidium; I/R, ischemia/reperfusion; NOX2, NADPH oxidase 2.

Antioxidant nanoparticles formulated from cerium, yttrium, and platinum have been reported to protect against the progression of cardiac dysfunction and remodeling by attenuation of myocardial oxidative stress and inflammatory processes, although there are concerns regarding their toxicity.²⁴⁻²⁶ Nanoparticle-based drug delivery systems have also been developed for targeted delivery of antioxidant therapeutics to reduce infarct volumes and provide sufficient cardioprotective effects during acute myocardial infarction.^{10,27} However, various antioxidant strategies failed to reveal their beneficial effects in the clinical setting, and their therapeutic effects were not clearly elucidated.

Ineffectiveness of antioxidant therapy could be explained by various reasons, such as incorrect dosing, dosing frequency, late administration, and inappropriate biomarkers of oxidative damage. However, one of the most likely reasons for the failure of antioxidant strategies for I/R injury could be the lack of interactions between the therapeutic antioxidant and the specific ROS driving the pathological conditions.⁸ In this context, scavenging of overproduced H₂O₂ in the site of oxidative stress is a logical strategy for effective treatment of myocardial I/R injury. In this present study we evaluated the potential of PVAX nanoparticles, which are rapidly activated by H₂O₂, to exert potent antioxidant, anti-inflammatory, and antiapoptotic activities during myocardial I/R. PVAX nanoparticles dramatically reduced the ROS-mediated oxidative stress and effectively attenuated I/R injury with reduction of infarct size and improvement of cardiac function.

The present study also demonstrated that PVAX nanoparticles effectively blocked NOX-derived ROS overproduction. It is well known that NOX2 and NOX4, electron-transporting membrane enzymes, are major components of the NOX isoforms that produce ROS, particularly superoxide anions and H₂O₂, in heart.²⁸ NOX2 is involved in cardiac remodeling after myocardial infarction, whereas NOX4 is a critical mediator of mitochondrial oxidative stress and mitochondrial dysfunction during heart failure.^{29,30} Previous studies reported that I/R induced significant increases in the levels of NOX2 and NOX4 expression.³¹ In addition, knockdown of NOX2 or NOX4 led to a significant decrease in the infarct size accompanied with decrease in cardiomyocyte apoptosis after I/R. We found that PVAX nanoparticles significantly reduced the level of NOX2 and NOX4 expression, which favors the reduction in ROS generation after I/R. The down-regulation of NOX2 and NOX4 may not reflect a true decrease in the activity of the NOXs to generate ROS. However, previous study showed that down-regulation of a single NOX is sufficient to achieve a >50% reduction of ROS.³¹ Altogether, blocking the undesirable actions of NOXs with PVAX nanoparticles could be a logical therapeutic strategy for treating oxidative stress-related pathologies such as I/R injury and neurodegenerative and metabolic diseases.

Sources of Funding

This work was supported in part by the grants from NIH 1 R44 DK103389-01 (P.M. Kang), Brain Korea 21 Plus program from Ministry of Education, Science and Technology, Korea, (D. Lee, P.M. Kang), Korea Health Technology R&D Project (HI13C1370) (D. Lee), and Handok Pharmaceuticals (P.M. Kang, S.U. Lee). S. Dilmen was supported by a Scientific and Technological Research Council of Turkey (TÜBİTAK) grant.

Disclosures

None.

References

1. Santiago E, Contreras C, Garcia-Sacristan A, Sanchez A, Rivera L, Climent B, Prieto D. Signaling pathways involved in the H₂O₂-induced vasoconstriction of rat coronary arteries. *Free Radic Biol Med*. 2013;60:136–146.
2. Taverne YJ, Bogers AJ, Duncker DJ, Merkus D. Reactive oxygen species and the cardiovascular system. *Oxid Med Cell Longev*. 2013;2013:862423.
3. Munzel T, Gori T, Bruno RM, Taddei S. Is oxidative stress a therapeutic target in cardiovascular disease? *Eur Heart J*. 2010;31:2741–2748.
4. Bolli R, Jeroudi MO, Patel BS, DuBose CM, Lai EK, Roberts R, McCay PB. Direct evidence that oxygen-derived free radicals contribute to postischemic myocardial dysfunction in the intact dog. *Proc Natl Acad Sci USA*. 1989;86:4695–4699.
5. Gottlieb RA, Bursleson KO, Kloner RA, Babior BM, Engler RL. Reperfusion injury induces apoptosis in rabbit cardiomyocytes. *J Clin Invest*. 1994;94:1621–1628.
6. Slezak J, Tribulova N, Pristacova J, Uhrik B, Thomas T, Khaper N, Kaul N, Singal PK. Hydrogen peroxide changes in ischemic and reperfused heart. Cytochemistry and biochemical and x-ray microanalysis. *Am J Pathol*. 1995;147:772–781.
7. Lee D, Khaja S, Velasquez-Castano JC, Dasari M, Sun C, Petros J, Taylor WR, Murthy N. In vivo imaging of hydrogen peroxide with chemiluminescent nanoparticles. *Nat Mater*. 2007;6:765–769.
8. Rosenbaugh EG, Savalia KK, Manickam DS, Zimmerman MC. Antioxidant-based therapies for angiotensin II-associated cardiovascular diseases. *Am J Physiol Regul Integr Comp Physiol*. 2013;304:R917–R928.
9. Kim KS, Khang G, Lee D. Application of nanomedicine in cardiovascular diseases and stroke. *Curr Pharm Des*. 2011;17:1825–1833.
10. Yun X, Maximov VD, Yu J, Zhu H, Vertegel AA, Kindy MS. Nanoparticles for targeted delivery of antioxidant enzymes to the brain after cerebral ischemia and reperfusion injury. *J Cereb Blood Flow Metab*. 2013;33:583–592.
11. Lee D, Bae S, Hong D, Lim H, Yoon JH, Hwang O, Park S, Ke Q, Khang G, Kang PM. H₂O₂-responsive molecularly engineered polymer nanoparticles as ischemia/reperfusion-targeted nanotherapeutic agents. *Sci Rep*. 2013;3:2233.
12. Lee D, Bae S, Ke Q, Lee J, Song B, Karumanchi SA, Khang G, Choi HS, Kang PM. Hydrogen peroxide-responsive copolyoxalate nanoparticles for detection and therapy of ischemia-reperfusion injury. *J Control Release*. 2013;172:1102–1110.
13. Yang J, Marden JJ, Fan C, Sanlioglu S, Weiss RM, Ritchie TC, Davison RL, Engelhardt JF. Genetic redox preconditioning differentially modulates AP-1 and NF kappa B responses following cardiac ischemia/reperfusion injury and protects against necrosis and apoptosis. *Mol Ther*. 2003;7:341–353.
14. Choudhury S, Bae S, Kumar SR, Ke Q, Yalamarti B, Choi JH, Kirshenbaum LA, Kang PM. Role of AIF in cardiac apoptosis in hypertrophic cardiomyocytes from Dahl salt-sensitive rats. *Cardiovasc Res*. 2010;85:28–37.
15. Jang YW, Lee JY, Kim CJ. Anti-asthmatic activity of phenolic compounds from the roots of *Gastrodia elata* Bl. *Int Immunopharmacol*. 2010;10:147–154.
16. Choudhury S, Bae S, Ke Q, Lee JY, Kim J, Kang PM. Mitochondria to nucleus translocation of AIF in mice lacking Hsp70 during ischemia/reperfusion. *Basic Res Cardiol*. 2011;106:397–407.
17. Pawlinski R, Tencati M, Hampton CR, Shishido T, Bullard TA, Casey LM, Andrade-Gordon P, Kotsch M, Spring D, Luther T, Abe J, Pohlman TH, Verrier

- ED, Blaxall BC, Mackman N. Protease-activated receptor-1 contributes to cardiac remodeling and hypertrophy. *Circulation*. 2007;116:2298–2306.
18. Wang JX, Jiao JQ, Li Q, Long B, Wang K, Liu JP, Li YR, Li PF. MIR-499 regulates mitochondrial dynamics by targeting calcineurin and dynamin-related protein-1. *Nat Med*. 2011;17:71–78.
 19. Brandes RP, Weissmann N, Schroder K. Redox-mediated signal transduction by cardiovascular NOX NADPH oxidases. *J Mol Cell Cardiol*. 2014;73:70–79.
 20. Meldrum DR, Dinarello CA, Cleveland JC Jr, Cain BS, Shames BD, Meng X, Harken AH. Hydrogen peroxide induces tumor necrosis factor alpha-mediated cardiac injury by a p38 mitogen-activated protein kinase-dependent mechanism. *Surgery*. 1998;124:291–296; discussion 297.
 21. Adlam VJ, Harrison JC, Porteous CM, James AM, Smith RA, Murphy MP, Sammut IA. Targeting an antioxidant to mitochondria decreases cardiac ischemia-reperfusion injury. *FASEB J*. 2005;19:1088–1095.
 22. Yarbrough WM, Mukherjee R, Stroud RE, Meyer EC, Escobar GP, Sample JA, Hendrick JW, Mingoia JT, Spinale FG. Caspase inhibition modulates left ventricular remodeling following myocardial infarction through cellular and extracellular mechanisms. *J Cardiovasc Pharmacol*. 2010;55:408–416.
 23. Guo J, Wang SB, Yuan TY, Wu YJ, Yan Y, Li L, Xu XN, Gong LL, Qin HL, Fang LH, Du GH. Coptisine protects rat heart against myocardial ischemia/reperfusion injury by suppressing myocardial apoptosis and inflammation. *Atherosclerosis*. 2013;231:384–391.
 24. Niu J, Azfer A, Rogers LM, Wang X, Kolattukudy PE. Cardioprotective effects of cerium oxide nanoparticles in a transgenic murine model of cardiomyopathy. *Cardiovasc Res*. 2007;73:549–559.
 25. Yamagishi Y, Watari A, Hayata Y, Li X, Kondoh M, Yoshioka Y, Tsutsumi Y, Yagi K. Acute and chronic nephrotoxicity of platinum nanoparticles in mice. *Nanoscale Res Lett*. 2013;8:395.
 26. Schubert D, Dargusch R, Raitano J, Chan SW. Cerium and yttrium oxide nanoparticles are neuroprotective. *Biochem Biophys Res Commun*. 2006;342:86–91.
 27. Chang MY, Yang YJ, Chang CH, Tang AC, Liao WY, Cheng FY, Yeh CS, Lai JJ, Stayton PS, Hsieh PC. Functionalized nanoparticles provide early cardioprotection after acute myocardial infarction. *J Control Release*. 2013;170:287–294.
 28. Joshi-Barr S, de Gracia Lux C, Mahmoud E, Almutairi A. Exploiting oxidative microenvironments in the body as triggers for drug delivery systems. *Antioxid Redox Signal*. 2014;21:730–754.
 29. Kuroda J, Ago T, Matsushima S, Zhai P, Schneider MD, Sadoshima J. NADPH oxidase 4 (NOX4) is a major source of oxidative stress in the failing heart. *Proc Natl Acad Sci USA*. 2010;107:15565–15570.
 30. Looi YH, Grieve DJ, Siva A, Walker SJ, Anilkumar N, Cave AC, Marber M, Monaghan MJ, Shah AM. Involvement of NOX2 NADPH oxidase in adverse cardiac remodeling after myocardial infarction. *Hypertension*. 2008;51:319–325.
 31. Matsushima S, Kuroda J, Ago T, Zhai P, Ikeda Y, Oka S, Fong GH, Tian R, Sadoshima J. Broad suppression of NADPH oxidase activity exacerbates ischemia/reperfusion injury through inadvertent downregulation of hypoxia-inducible factor-1alpha and upregulation of peroxisome proliferator-activated receptor-alpha. *Circ Res*. 2013;112:1135–1149.